IEEE Access
Multidisciplinary ⋮ Rapid Review ⋮ Open Access Journal

Received October 23, 2019, accepted November 5, 2019, date of publication November 8, 2019, date of current version November 20, 2019.

Digital Object Identifier 10.1109/ACCESS.2019.2952358

Decomposed-Coordinated Framework With Enhanced Extremum Kriging for Multicomponent Dynamic Probabilistic Failure Analyses

CHENG LU[1], YUN-WEN FENG[1], CHENG-WEI FEI[2], AND SIQI BU[3], (Senior Member, IEEE)

[1]School of Aeronautics, Northwestern Polytechnical University, Xi'an 710072, China
[2]Department of Aeronautics and Astronautics, Fudan University, Shanghai 200433, China
[3]Department of Electrical Engineering, The Hong Kong Polytechnic University, Hong Kong

Corresponding author: Cheng-Wei Fei (cwfei@fudan.edu.cn)

This work was supported in part by the National Natural Science Foundation of China under Grant 51875465 and Grant 51975124, in part by the Research Start-Up Funding of Fudan University under Grant FDU38341, in part by the Innovation Foundation for Doctor Dissertation of Northwestern Polytechnical University under Grant CX201932, and in part by The Hong Kong Polytechnic University Start-Up Fund under Grant 1-ZE68.

ABSTRACT For multicomponent structures enduring dynamic workloads coming from multi-physical fields, safety assessment is significant to guarantee the normal operation of entire structure system. In this paper, an enhanced extremum Kriging-based decomposed coordinated framework (E2K-DCF) is proposed to improve the dynamic probabilistic failure analyses of multicomponent structures. In this method, extremum Kriging model (EKM) is developed by introducing Kriging model into extremum response surface method (ERSM) to process the transient response problem and shorten computational burden in dynamic probabilistic failure analyses. Multiple population genetic algorithm (MPGA) is employed to solve maximum likelihood equation (MLE) and find the optimal hyperparameter $\boldsymbol{\theta}$ in the EKM, which is promising to enhance approximate accuracy; decomposed-coordinated (DC) strategy is used to handle the coordinated relationship of multiple analytical objectives. To validate the proposed E2K-DCF, the probabilistic failure analysis of turbine blisk radial deformation is conducted by comparing with different methods within time domain [0 s, 215 s], considering fluid-thermal-structural interaction. It is revealed that the failure probability of blisk radial deformation is only 0.0022 when the allowable value is 2.5702×10^{-3} m acquired from real world practice. Compared to the other approaches, this E2K-DCF has obvious advantages in fitting time and accuracy as well as simulation efficiency and accuracy. The results illustrate that the E2K-DCF is effective and applicable in dynamic probabilistic failure analysis. The efforts of this paper provide a novel viewpoint for the transient reliability evaluation of multicomponent structures, which is likely to enrich mechanical reliability theory.

INDEX TERMS E2K-DCF, multicomponent structure, multiple population genetic algorithm, probabilistic failure, turbine blisk.

I. INTRODUCTION

Complex structure in gas turbine always involves multiple components and endures complicated workloads induced by multi-physical fields during operation [1]. The complex structure involving multiple components is called as multicomponent structure. When one component occurs failure, the multicomponent structure cannot function properly and even a catastrophic event emerges during operation [2]. For complex machine, in fact, the factors or parameters influencing the structure hold naturally randomness and time-varying feature in operation. To guarantee the safety and performance of the structure, it is urgent to investigate the probabilistic failure analysis of multicomponent structures considering the effect of dynamic loads and the randomness of influencing parameters.

With the development of structural probabilistic failure analysis, various approaches have emerged. Azizsoltani, et al., discussed the structural reliability estimation of engineering systems by adopting Monte Carlo (MC) simulation

The associate editor coordinating the review of this manuscript and approving it for publication was Dong Wang.

and Gaussian process regression active learning [3]. Zhan, *et al*., presented continuum damage mechanics based approach for the fatigue life evaluation of scarf bolted joints [4], [5]. Liu, *et al*., used first order second moment (FOSM) method to evaluate the chatter reliability of milling system [6]. Adarsh, *et al*., studied the probabilistic failure analysis of composite channels with advanced FOSM method and MC simulation [7]. Du, *et al*., applied first order reliability method and saddlepoint approximation to discuss structural reliability degree on the premise of guaranteeing computational efficiency [8]. Zhao, *et al*., investigated the first order third moment reliability method to calculate failure probability of mechanical structures [9]. Zhang, *et al*., exploited second order reliability method with first order efficiency to assess structural failure probability [10]. Zhu, *et al*., discussed the fatigue reliability assessment of gas turbine discs/bladed disks based on finite element (FE)-based computational and experimental methods [11]–[13]. Lu, *et al*., proposed a second order fourth moment method for the failure probability estimation of mechanical structures [14]. Despite the aforementioned methods are effective in structural probabilistic failure analysis, they cannot be applied to the dynamic reliability analyses of multicomponent structures, due to the required thousands of iterations for real models.

To address the above issue, a number of analytical approaches emerged for structural dynamic probabilistic analysis. Guerine, *et al*., proposed an interval analysis method for the dynamic probabilistic failure analysis of wind turbine gear [15]. Codetta-Raiteri, *et al*., used dynamic Bayesian networks for structural reliability evaluation regarding dynamic loads [16]. Mo, studied structural dynamic failure analysis using perturbation stochastic finite element with stress-strength interference model [17]. In addition, some effective methods based on surrogate models such as response surface method (RSM), Kriging meta-model, artificial neural network, support vector machine, and so forth, were recently applied to structural dynamic probabilistic failure analysis. Li, *et al*., investigated t a sequential surrogate method for reliability analysis based on radial basis function [18]. Bai, *et al*., employed the extremum RSM (ERSM) to assess the dynamic reliability of turbine blisk [19]. Cheng, *et al*., employed adaptive Kriging meta-model to the structural comprehensive performance evaluation with dynamic characteristics [20]. Soltani, *et al*., explored a novel approach for reliability investigation of LEDs on molded interconnect devices based on FE-analysis coupled to injection molding simulation [21]. Fei, *et al*., quantified the transient failure probability of turbine blade deformation with support vector machine-based ERSM [22]. Although the above approaches can be applied to structural reliability analysis with regard to dynamic boundary, it is insufficient yet to resolve the dynamic probabilistic analysis of multicomponent structures. Furthermore, Fei *et al*. offered a distribution collaborative ERSM for the dynamic probabilistic analysis for turbine blade-tip radial clearance [23]. However, the improved surrogate modeling strategy still suffers from low approximate accuracy and low simulation performance, owing to the limitation quadratic polynomials (QP) and the thousands of structural dynamic deterministic analyses. Therefore, we need to explore an efficient and precise technique to perform the dynamic probabilistic analysis of multicomponent structures.

The objective of this paper is to provide an enhanced extremum Kriging-based decomposed-coordinated framework (E2K-DCF) for multicomponent structural probabilistic failure analysis with dynamic loads and random parameters, by integrating the strengths of Kriging model, ERSM, multiple population genetic algorithm (MPGA) and decomposed-coordinated (DC) strategy. Herein, ERSM is introduced into Kriging model, named as extremum Kriging model (EKM), to alleviate computational burden and improve approximate accuracy. MPGA is adopted to resolve the maximum likelihood equation (MLE) rather than gradient descent optimizer to search the hyperparameter $\boldsymbol{\theta}$ in the EKM. The DC strategy is to coordinate the relationship of multiple components. To validate the developed method, the dynamic probabilistic failure analysis of turbine blisk is conducted to verify the proposed approach in engineering, by considering fluid-thermal-structural interaction.

In what follows, Section II elaborates the basic principles of E2K-DCF. In Section III, we discuss the dynamic probabilistic failure analysis with the proposed method. Section IV validates the developed E2K-DCF via the dynamic probabilistic failure analysis of turbine blisk radial deformation. Some conclusions are summarized in Section V.

II. THEORY AND METHODS

This section investigates the related theory and methods including EKM, MPGA, E2K-DCF and the dynamic probabilistic failure analysis procedure of multicomponent structures with E2K-DCF.

A. EXTREMUM KRIGING MODEL

Kriging model holds good approximate performance in prediction, and thus is widely applied in performance analysis [20], [24], probabilistic failure analysis [25], [26], sensitivity assessment [27], [28], and design optimization [29], [30], for structure system. However, Kriging model is inefficient for dynamic structural probabilistic analysis, because multiple models are required modeling for dynamic operational process and greatly enlarge computational complexity and consumptions. To resolve this issue, ERSM was proposed to reduce computational burden by considering the extreme value of output response process instead of the whole process in time domain $[0, T]$ [31], [32]. However, this model still faces the challenge of approximate accuracy for large-scale parameters and high-nonlinear problem because of the limitation of quadratic polynomial. To overcome the two defects, we develop extremum Kriging model (EKM) for structural dynamic probabilistic failure analyses by absorbing the superiorities of ERSM and Kriging model. Thereinto, the ERSM is used to resolve the dynamic response problem in respect of the extremum values, and Kriging model

is employed to improve the prediction accuracy. Therefore, regarding Kriging model and ERSM, EKM model can be expressed as

$$y_{EKM}(\boldsymbol{x}) = y_{ERSM}(\boldsymbol{x}) + z(\boldsymbol{x}) \tag{1}$$

which contains two parts, i.e., an ERSM model $y_{ERSM}(\boldsymbol{x})$ and a realization $z(\boldsymbol{x})$ of stochastic process that is to amend the error between predicted value with ERSM model and true value; $\boldsymbol{x} \in R^m$ denotes the data to be predicted where m is the number of dimensions (i.e., the number of input parameters).

Assuming that $\{y_{l,\max}(\boldsymbol{x}_l)\}_{l=1,2,\ldots,n}$ is the set of the extreme values of dynamic response process in time domain, the ERSM function y_{ERSM} can be fitted as

$$y_{ERSM}(\boldsymbol{x}) = \left\{y_{l,\max}(\boldsymbol{x}_l)\right\}_{l=1,2,\cdots n} \tag{2}$$

where n is the number of samples; the symbol $y_{l,\max}(\boldsymbol{x}_l)$ indicates the extreme value of l-th transient output response y_l in time domain $[0, T]$ corresponding to l-th sample $\boldsymbol{x}_l$.

Regarding quadratic polynomial, the ERSM function is written as

$$y_{ERSM}(\boldsymbol{x}) = \boldsymbol{a} + \boldsymbol{b}\boldsymbol{x} + \boldsymbol{x}^T\boldsymbol{c}\boldsymbol{x} \tag{3}$$

where a is constant coefficient; $\boldsymbol{b}$ is vector of linear term;$\boldsymbol{c}$ is matrix of quadratic term.

The second term $z(\boldsymbol{x})$ is a stationary Gaussian random function and obeys

$$\begin{cases} E[z(\boldsymbol{x})] = 0 \\ Var[z(\boldsymbol{x})] = \sigma^2 \\ Cov\left[z(\boldsymbol{x}_p), z(\boldsymbol{x}_q)\right] = \sigma^2 R(\boldsymbol{\theta}, \boldsymbol{x}_p, \boldsymbol{x}_q) \end{cases} \tag{4}$$

here the symbols $\boldsymbol{x}_p$ and $\boldsymbol{x}_q$ indicate the vectors of p-th and q-th input samples($p, q = 1, 2, \ldots, n$); σ^2 is the process variance; $R(\cdot)$ denotes spatial correlation function (SCF) with $R(0) = 1$; $\boldsymbol{\theta} = [\theta_1, \theta_2, \ldots, \theta_m]$ represents correlation parameter vector to be estimated by R. The hyperparameters $\boldsymbol{\theta}$ are called as distance weights or length scales, which is typically obtained by solving MLE with gradient descent optimizer. In engineering, Gaussian correlation function is generally regarded as the SCF to find the optimal parameters in Kriging model, because Gaussian function can enhance the Kriging modelling of high dimensional problem in computational efficiency and accuracy by effectively reducing dimensions [25], [32]. The Gaussian correlation function $R(\cdot)$ in Eq.(4)is expressed in Eq. (5).

$$\begin{aligned} R(\boldsymbol{\theta}, \boldsymbol{x}_p, \boldsymbol{x}_q) &= \prod_{i=1}^{m} \exp\left(-\theta_i \left|x_p^i - x_q^i\right|^2\right) \\ &= \exp\left(-\sum_{i=1}^{m} \theta_i \left|x_p^i - x_q^i\right|^2\right) \end{aligned} \tag{5}$$

in which x_p^i and x_q^i are i-th component of p-th and q-th input samples; $\left|x_p^i - x_q^i\right|$ represents the distance between p-th and q-th points in i-th dimension; θ_k describes the sensitivity of output response with respect to i-th dimensional input variation x^i, which controls the characteristics of inputs and outputs to ensure the prediction accuracy of model via optimal solution.

To gain the hyperparameter $\boldsymbol{\theta}$, we usually employ the gradient descent optimizer to maximize the MLE, i.e.,

$$\Psi(\boldsymbol{\theta}) = -\left(n \ln \hat{\sigma}^2 + \ln |\boldsymbol{R}|\right) \tag{6}$$

With regard to the gradient descent optimizer [25], the hyperparameter $\boldsymbol{\theta}_{gdo}$ can be gained as

$$\begin{aligned} \boldsymbol{\theta}_{gdo} &= \arg\max\{\Psi(\boldsymbol{\theta})\} \\ &= \arg\max\left\{-\left(n \ln \hat{\sigma}^2 + \ln |R|\right)\right\} \end{aligned} \tag{7}$$

where $\boldsymbol{R}$ is $n \times n$ correlation matrix which is a positive semidefinite matrix since the SCF defines all elements as positive semidefinite; $\hat{\sigma}^2$ is the estimated variance.

In line with the acquired the hyperparameter $\boldsymbol{\theta}_{gdo}$, we can gain the stochastic process $z(\boldsymbol{x})$ and then derive EKM model Eq.(1) together with ERSM model Eq.(3).

B. ENHANCED EXTREMUM KRIGING MODEL

The hyperparameters $\boldsymbol{\theta}$ is the key factor of affecting the modeling accuracy of EKM. When the gradient descent optimizer approach is applied to resolve the MLE and to obtain the hyperparameters $\boldsymbol{\theta}$ for traditional Kriging model, it is required to implement numerous iterations for the large-scale parameters and high-nonlinear problems, and the results also easy immerses in local optimum. To overcome this problem, genetic algorithm (GA) was applied to find the optimal values of hyperparameter $\boldsymbol{\theta}$, which was demonstrated to have better advantages than gradient descent optimizer, owing to strong robustness and global search ability [33]. However, we find that the GA exist premature problem due to fitness value, crossover and mutation probabilities, population size, termination criterion and so forth [34].

To address the above issue, we attempt to adopt the MPGA to search the optimal values of hyperparameters $\boldsymbol{\theta}$. Relative to the GA, the MPGA holds flexible and adaptive design space exploration, and avoid the influence of the plateau-like function profile of MLE. Besides, the MPGA uses multiple populations with different control parameters for optimization iterations which can breaks the limitation of single population evolution of GA in premature problem [35], [36]. Substantially, MPGA originates from GA and inherits natural selection and genetic characteristics. And the optimal solution of objective function can be gained via successive iterations with selection, crossover and mutation. The schematic diagram of MPGA is shown in Fig. 1.

As shown in Fig. 1, N initial populations with binary encoding are firstly generated. Then N new populations are obtained by the procedures of selection operator, crossover operator and mutation. We further select the optimal individuals of each excellent population via artificial selection operator to structure elite population for searching the optimal value of objective function. Obviously, the MPGA is essentially a combination of multiple GAs, and different

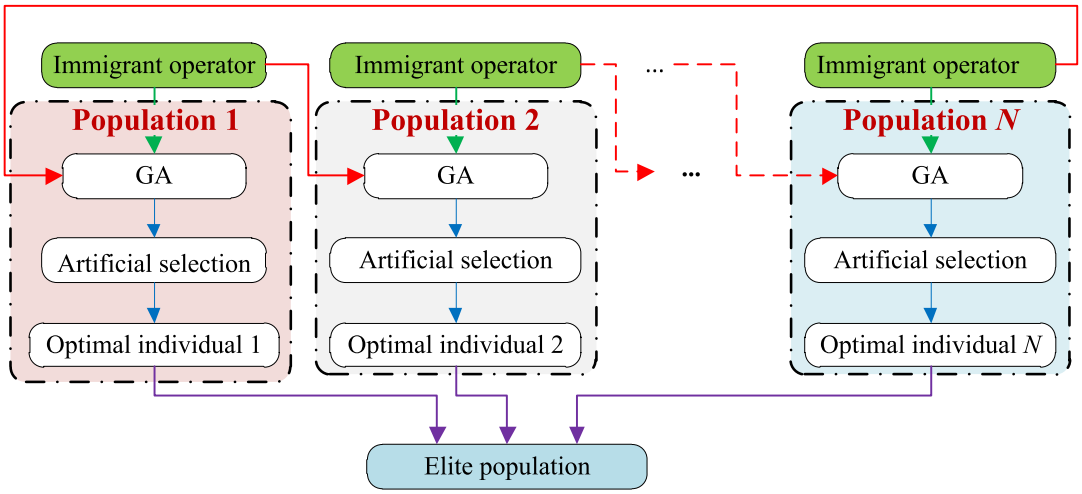

FIGURE 1. The schematic diagram of MPGA.

control parameters (i.e., crossover probability $p_{c,l}$ and mutation probability $p_{m,l}$) are used to complete the collaborative evaluation of multiple populations ($l = 1, 2 \ldots, N$). Meanwhile, immigrant operator [8], [15] is introduced to exchange message among populations, and to avoid the destruction and loss of optimal individual information. In the exchange, the elite population doesn't participate selection, crossover and mutation operators, and the minimum reserved generation is usually regarded as the terminal condition of optimization iterations. Obviously, the MPGA have global search and local search ability, as well as avoid the phenomenon of premature.

For an optimal problem, the objective function is built as

$$\varphi(\boldsymbol{\theta}) = |\boldsymbol{R}|^{\frac{1}{n}} \hat{\sigma}^2 \tag{8}$$

By minimizing objective function with MPGA, the hyperparameter $\boldsymbol{\theta}_{MPGA}$ is gained as

$$\begin{aligned} \boldsymbol{\theta}_{MPGA} &= \min\{\varphi(\boldsymbol{\theta})\} \\ &= \min\left\{|\boldsymbol{R}|^{\frac{1}{n}} \hat{\sigma}^2\right\}_{\theta^i>0, i=1,2,\cdots,m} \end{aligned} \tag{9}$$

The EKM of finding the hyperparameters θ by MPGA is called as enhanced EKM (E2K model, short for). In term of Eqs. (1) and (9), the E2K model is structured as

$$y_{E2K}(\boldsymbol{x}) = y_{ERSM}(\boldsymbol{x}) + z_{MPGA}(\boldsymbol{x}) \tag{10}$$

C. ENHANCED EXTREMUM KRIGING-BASED DECOMPOSED-COORDINATED FRAMEWORK

For the probabilistic failure evaluation of multicomponent structure involving many parts, E2K model is workable if it is directly applied, because this analysis has excess computational burden and unacceptable accuracy for high nonlinearity and hyperparameters. To address this problem, we absorb the basic thought of DC strategy to divide the whole structure into multiple components, and firstly perform their analyses with E2K models and then coordinate their responses to process the probabilistic analysis of multicomponent structure. The framework commonly includes three layers, i.e., structure layer, substructure layer and variable layer. Obviously, the DC strategy is promising to effectively reduce the nonlinearity and parameter size for probabilistic analyses, which skillfully relieve the computational burden and improve computing accuracy [37]. Along with the heuristic thought, the DC strategy and the E2K model are integrated to develop E2K-based DC framework (E2K-DCF), for the dynamic probabilistic failure analyses of multicomponent structure.

When multicomponent structure consists of k ($k \in Z$) substructures, the coordinated surrogate models between structure and substructures are established as

$$y_{E2K-DCF}(\boldsymbol{x}) = f\left(y_{E2K}^{(1)}\left(\boldsymbol{x}^{(1)}\right), \cdots, y_{E2K}^{(k)}\left(\boldsymbol{x}^{(k)}\right)\right) \tag{11}$$

where $f(\cdot)$ denotes the function of multicomponent structure layer; $y_{E2K}^{(k)}\left(\boldsymbol{x}^{(k)}\right)$ is the decomposed surrogate model of k-th substructure; $\boldsymbol{x} = \left\{y_{E2M}^{(k)}\left(\boldsymbol{x}^{(k)}\right)\right\}$ is the coordinated input variables of the structure; $\boldsymbol{x}^{(k)} = \left[x_1^{(k)}, x_2^{(k)}, \cdots, x_l^{(k)}\right]^T$ is the input parameter related to k-th substructure.

In respect of ERSM model and MPGA, the k-th decomposed E2K model is

$$y_{E2K}^{(k)}\left(\boldsymbol{x}^{(k)}\right) = y_{ERSM}^{(k)}\left(\boldsymbol{x}^{(k)}\right) + z_{MPGA}^{(k)}\left(\boldsymbol{x}^{(k)}\right) \tag{12}$$

The relationship between $\boldsymbol{x}$ for structure system and $\{\boldsymbol{x}^{(l)}\}_{l=1,2,\ldots,k}$ for l-th substructure can be expressed as

$$\boldsymbol{x} = \bigcup_{l=1}^{k} \boldsymbol{x}^{(l)} \tag{13}$$

In line with the above analysis, the models of E2K-DCF including coordinated model (Eq. (11)) and decomposed models (Eq. (12)) are obtained.

To ensure the effectiveness of E2K-DCF modeling, the S-Fold Cross Validation (SF-CV) is employed to evaluate the modeling accuracy using training samples, by comparison of different approaches [38]. The procedure of SF-CV is shown as follows: the training samples are first separated into

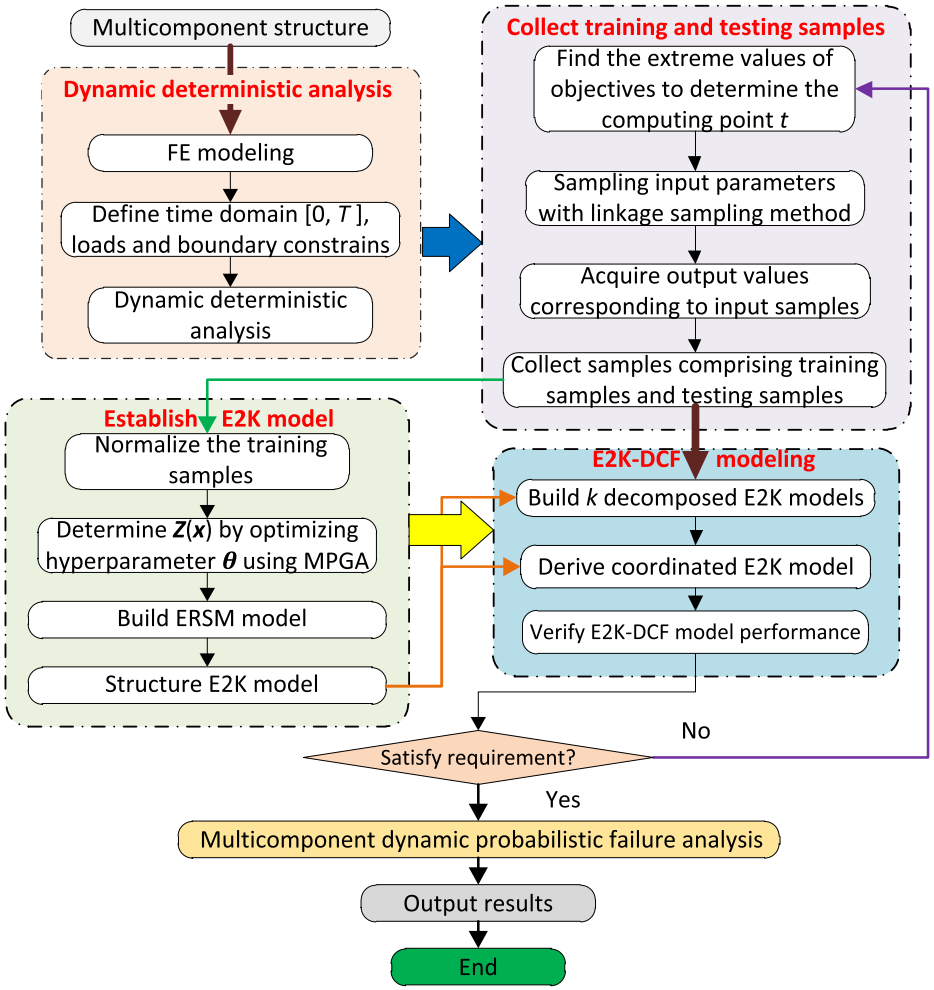

FIGURE 2. The procedure of multicomponent dynamic probabilistic failure analysis with E2K-DCF.

S groups randomly and averagely, in which S can be 5, 10 or 15; we then derive the models of E2K-DCF with the samples of S-1 groups, and the remaining samples are used to assess the merits and demerits of this model via root mean square error (RMSE), which is shown in Eq. (14); the mean value of RMSE with S iterations is obtained to assess the accuracy of surrogate models.

$$RMSE = \left(\frac{\sum_{l'=1}^{n'} \left(F_{l'}\left(\boldsymbol{x}\right) - u_{l'}\left(\boldsymbol{x}\right) \right)}{n'} \right) \tag{14}$$

in which $l' = 1, 2, \ldots, n'$, n' is the number of samples of each group; $F'_l(\boldsymbol{x})$ is the l'-th output response obtained by the direct simulation with full FE models; $y_{l'}(\boldsymbol{x})$ is l'-th output response computed by different methods.

Based on the determined model of E2K-DCF, we further apply absolute error $E_{ab,l''}$ and average absolute error E_{av} to validate the superiority of this model in term of computational accuracy, by using testing samples. $E_{ab,l''}$ and E_{av} are defined by

$$\begin{aligned} E_{ab,l''} &= \left| F_{l''}\left(\boldsymbol{x}\right) - y_{l''}\left(\boldsymbol{x}\right) \right| \\ E_{av} &= \sum_{l''=1}^{n''} E_{ab,l''}/n \end{aligned} \tag{15}$$

where $l'' = 1, 2, \ldots, n''$, n'' is the number of testing samples; $F_{l''}(\boldsymbol{x})$ and $y_{l''}(\boldsymbol{x})$ denote the output response obtained by the direct simulation and different surrogate modeling methods, corresponding to l''-th testing sample.

The dynamic probabilistic failure evaluation of multicomponent structure is performed with the derived model of E2K-DCF. Simultaneously, we use some surrogate modeling methods to implement the multicomponent dynamic probabilistic failure analyses by dividing a multicomponent structure into many substructures to reduce modelling dimension and parameter scale, to demonstrate the E2K-DCF in reducing computational burden and improving accuracy.

D. DYNAMIC PROBABILISTIC FAILURE ANALYSIS PROCEDURE FOR MULTICOMPONENT STRUCTURE

In respect of the E2K-DCF, the dynamic probabilistic failure analysis of multicomponent structure is shown in Fig. 2.

As illustrated in Fig. 2, the analytical process with E2K-DCF comprises dynamic deterministic analysis, samples collection, hyperparameters optimization in E2K model, E2K-DCF modeling and dynamic probabilistic failure analysis.

In respect of engineering practice, we establish the 3-dimension FE models of multicomponent structures. By defining time domain $[0, T]$, related load and boundary constrains, dynamic deterministic analysis is implemented with the FE models.

According to the analyses, the extreme values of analytical objectives are selected at the specified time point $t(t \in [0, T])$. At this point, we then generate samples of input parameters with regard to their numerical characteristics, using the linkage sampling method [33], [39], and then acquire the output samples in light of the deterministic analyses. Finally, the samples containing training samples and testing samples are structured for modeling. Hereinto, the linkage sampling method is to achieve the output responses for one sample simultaneously. Obviously, this sampling strategy can enhance the efficiency and reduce the burden in surrogate modeling process due to the synchronicity of sampling.

For confirming hyperparameters in E2K modeling, we normalize the data of training samples, and define the allowable parameters $\boldsymbol{\theta}^{(k)}$, and objective functions. Then the MPGA is applied to search for the optimal hyperparameter $\boldsymbol{\theta}$ in E2K models (i.e., decomposed surrogate models) with iterations. It is important to note that the training samples are separated into S groups randomly and averagely during the process of MPGA optimization, to obtain different Kriging hyperparameters with respect to different training samples, and the SF-CV is utilized to evaluate the accuracy of E2K-DCF modeling with the mean value of RMSE.

Using the obtained hyperparameter $\boldsymbol{\theta}^{(k)}$, the undetermined coefficients are computed and the decomposed E2K models of multicomponent structure are built, to derive the coordinated E2K model with respect to the relationship among multiple substructures.

The testing samples are adopted to verify the modelling performance of E2K-DCF. If not satisfy the accuracy requirement, new training samples are generated for model updating until the accuracy is acceptable.

With the derived model of E2K-DCF, the dynamic probabilistic failure analysis of multicomponent structure is performed.

E. TRANSIENT PROBABILISTIC APPROACH

For dynamic probabilistic analyses of multicomponent structures, the limit state function is established based on E2K models. The allowance value of analytical objective $y_{allow}(\boldsymbol{x})$, i.e.,

$$\begin{aligned} h(\boldsymbol{x}) &= y_{allow}(\boldsymbol{x}) - y_{E2K-DCF}(\boldsymbol{x}) \\ &= y_{allow}(\boldsymbol{x}) - f\left(y_{E2K}^{(1)}\left(\boldsymbol{x}^{(1)}\right), \cdots, y_{E2K}^{(k)}\left(\boldsymbol{x}^{(k)}\right)\right) \end{aligned} \tag{16}$$

where this multicomponent structure is safe when $h(\boldsymbol{x}) > 0$, while it is failed as $h(\boldsymbol{x}) < 0$.

FOSM method and MC method are commonly employed to handle dynamic probabilistic evaluation. Although the FOSM method is widely applied to investigate structural reliability analysis [5], [11], [40], it is unable to effectively resolve large-scale parameters and high-nonlinear problem yet, as the computational burden becomes onerous with the increasing parameters and dimensions. To avoid the existing shortcoming, MC method is applied to perform the dynamic probabilistic analysis of multicomponent structure, resulting from high efficiency and accuracy in determining limit state function of complex structure. Besides, the convergence of this method dependents on the number of simulations, and is not affected by the dimension of parameters [25], [41].

With Chebyshev theorem and Bemoulli theorem, the reliability and failure probabilities are achieved, i.e.,

$$\begin{aligned} p_r &= p(h(\boldsymbol{x}) > 0) \approx N_r / N_{total} \\ p_f &= p(h(\boldsymbol{x}) \le 0) \approx N_f / N_{total} \end{aligned} \tag{17}$$

where $N_{total} = N_r + N_f$ is the total number of simulations; N_r is the number of failure simulations; N_f is the number of safe simulations; p_r is safety probability; p_f is failure probability; $p(\cdot)$ is probability function.

In view of the above analysis, we can derive the limit state function for multicomponent structure, the failure probability and reliability degree are computed by the MC method.

III. DYNAMIC PROBABILISTIC FAILURE ANALYSIS OF TURBINE BLISK

Turbine blisk comprises one whole disk and 48 blades, which is typically- axisymmetric structure. To reduce simulation consumption, we only study 1/48 model with 1/48 disk and one blade. The 3D models of the blisk and flow field were generated in Fig. 3 and Fig. 4 by using Spaceclaim software.[1] By ANSYS Meshing,[2] the 3D FE/Finite Volume (FV) models of turbine blisk and flow field were gridded in Figs. 5, in which the blade has 75 097 nodes and 48 551 elements, the disk has 57 213 nodes and 33 885 elements, and flow field has 472 930 nodes and 338 917 elements, respectively. FTSI surface denotes fluid-thermal-structural interaction surface which is to deliver fluid and heat workloads to structure models.

The mission profile of aeroengine from start to cruise phase within time domain [0 s, 215 s] is selected to simulate the operation states of a turbine blisk [42], [43]. Fig. 6 defines 12 time points as computing points, which shows the variations of inlet velocity, rational speed and gas temperature with time. The material of turbine blisk is Nickel-based superalloy, GH4133B, with the density of 8.560×10^3 kg/m^3, Poisson's ratio of 0.3224 and modulus of elasticity of 161 GPa.

Since material and operational parameters have natural randomness in engineering, in accordance with engineering experience we select five parameters (i.e., inlet velocity v, outlet pressure P_{out}, gas temperature T_g, rational speed w and material density ρ) as random input parameters,

[1] http://www.spaceclaim.com/en/default.aspx
[2] https://www.ansys.com/products/platform/ansys-meshing

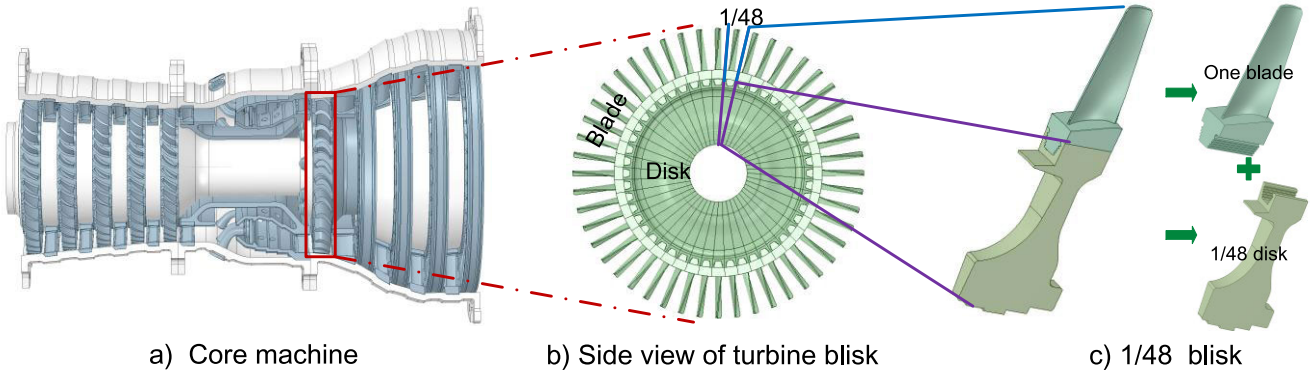

FIGURE 3. 3-D model of turbine blisk.

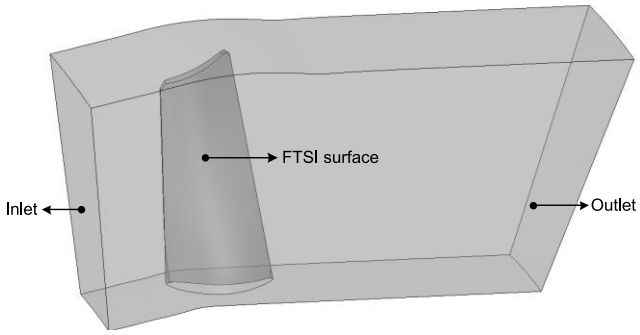

FIGURE 4. 3D model of flow field.

while the other parameters including Poisson's ratio, modulus of elasticity, and so forth, are regarded to be deterministic. For the random inputs, their features such as mean, standard deviation (Std. Dev.) and distribution types, are determined by the extremum selection method [44]. In respect of engineering practices [19], the random variables are considered to be normal distribution, for reducing the complexity of analysis [45], [46]. The distribution features of all random inputs are listed in Table 1.

A. DYNAMIC DETERMINISTIC ANALYSIS OF TURBINE BLISK

Under workbench environment of ANSYS (15.0 version), blisk radial deformation is deterministically investigated in [0 s, 215 s], by FE modeling and fluid-thermal-structural coupling. In fluid-thermal-structural coupling analysis, the close-coupling analysis method [33] is employed to implement the radial deformation analyses of turbine blisk in [0 s, 215 s], by Multiphysics Simulation module[3] [47], [48]. We decompose the fluid-thermal-structural system into three subsystems such as fluid, thermal and structural system. In other words, the dynamic deterministic analysis of blisk radial deformation is carried out by operating three subsystems separately with the standard k-ε turbulence model, employ the law of energy conservation to complete thermal analysis,

[3]https://www.ansys.com/products/platform/multiphysics-simulation

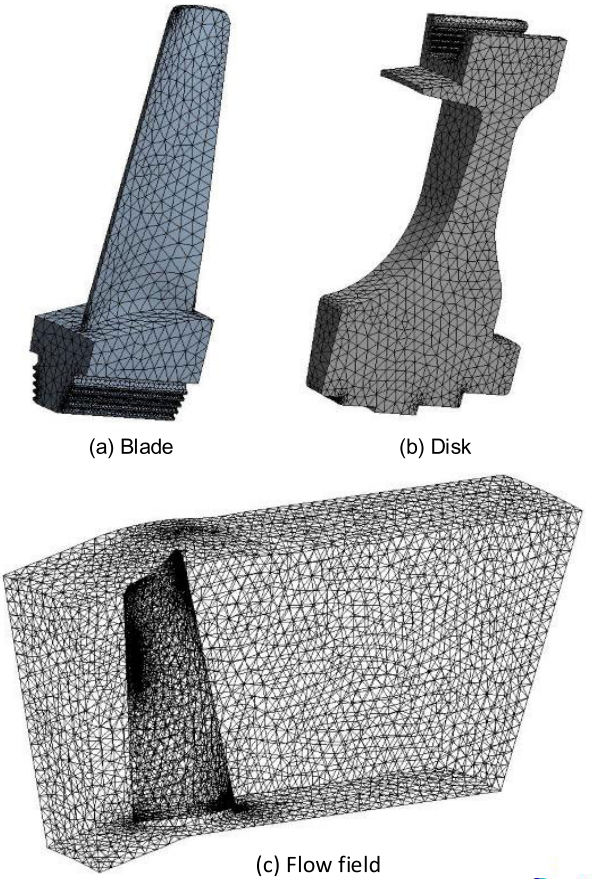

FIGURE 5. FE/FV models of turbine blisk and flow field.

and apply FE method to achieve turbine blisk analyses with tetrahedron shape equation and geometric equation. Regarding the deterministic analysis, therefore, the variations of blade and disk radial deformations with time are drawn in Fig. 7.

As illustrated in Fig. 7, the values of blade and disk (blisk) radial deformation become larger with the increasing inlet velocity, gas temperature and rational speed. The maximum values emerge in climb phase. In this case, we chose $t = 200$ s as the study point to perform the dynamic

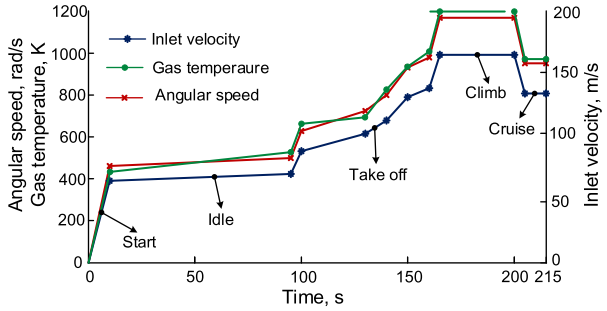

FIGURE 6. Change curves of inlet velocity, rational speed and gas temperature with time.

TABLE 1. Distribution features of random input parameters.

Input parameter	Distributions	Features	
		Mean	Std. Dev.
Inlet velocity v, m/s	Normal	160	8
Outlet pressure P_{out}, Pa	Normal	588000	58800
Gas temperature T_g, K	Normal	1200	72
Rational speed w, rad/s	Normal	1168	58.4
Material density ρ, kg/m^3	Normal	8560	770.4

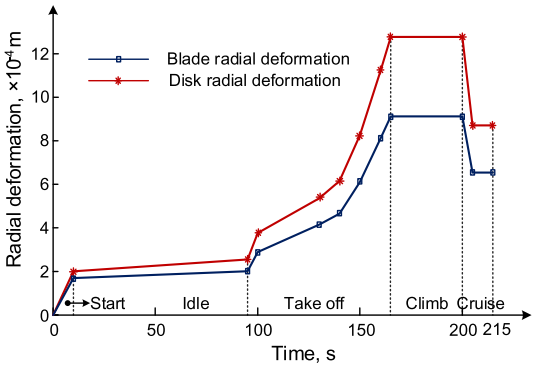

FIGURE 7. Variation of turbine blisk radial deformation within time domain [0 s, 215 s].

probabilistic failure analysis of turbine blisk radial deformation. Moreover, the distribution contour plots for the pressure of FTSI surface, temperature and radial deformation of turbine blisk at this study point are displayed in Fig. 8 and Fig. 9, respectively. Herein, P is pressure value in FTSI surface; T_b denotes temperature on surface of turbine blisk; u_b and u_d are the radial deformations of turbine blade and disk.

B. DYNAMIC PROBABILISTIC FAILURE ANALYSIS OF TURBINE BLISK

For the dynamic probabilistic failure analyses of turbine blisk radial deformation with E2K-DCF, a pool of 150 input samples was firstly gained with the linkage sampling method in line with the distribution features of input variables in Table 1, and then the output responses (the radial deformation of blade and disk) corresponding to the extracted input samples were computed in respect of dynamic deterministic analyses introduced in Part B of Section III. The acquired 150 input samples

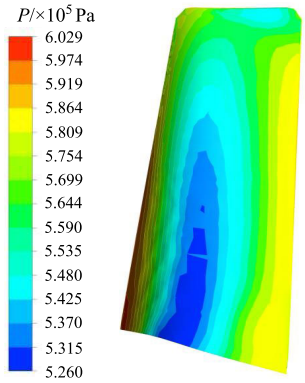

(a) Pressure distribution of FTSI surface

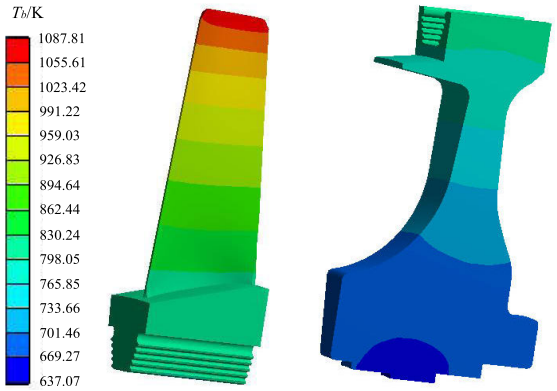

(b) Temperature distribution of blade and disk

FIGURE 8. Pressure and temperature distribution at t = 200 s.

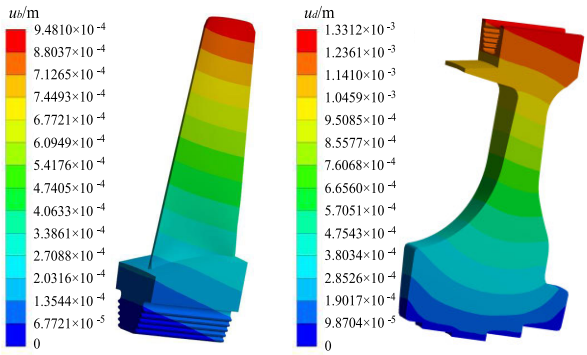

(a) Radial deformation for turbine blade (b) Radial deformation for turbine disk

FIGURE 9. Radial deformation of turbine blisk at t = 200 s.

and 150 output samples were integrated as the 150 samples for dynamic probabilistic failure analyses later. In the pool of 150 samples, 50 samples were opted as training samples for E2K modeling for decomposed- and coordinated-surrogate models, and the remaining 100 samples were regarded as testing samples for validating the fitted models. In this case study, we divide the training samples into 5 groups, namely $S = 5$, to establish the surrogate models of study objectives, by using the E2K-DCF, ERSM-based DC strategy (DCERSM) and improved extremum Kriging (IEK)-based DC strategy (DCIEKS) [33], [42]. Here, the DCERSM was

TABLE 2. The results of 5 cross validations with 50 training samples using DCERSM, DCIEKS and E2K-DCF.

Group	DCERSM		DCIEKS		E2K-DCF	
no.	$RMSE_b$	$RMSE_d$	$RMSE_b$	$RMSE_d$	$RMSE_b$	$RMSE_d$
1	0.79	1.24	0.66	0.81	0.49	0.72
2	1.28	1.61	0.87	0.95	1.07	0.84
3	0.86	0.94	0.62	0.73	0.47	0.62
4	1.38	1.14	0.84	0.93	0.83	0.76
5	1.55	1.37	1.33	1.24	1.25	1.13
Mean	**1.17**	**1.26**	**0.86**	**0.93**	**0.82**	**0.81**

developed by integrating DC strategy and ERSM in respect of quadratic polynomials; the DCIEKS was proposed by absorbing DC strategy and IEK method, in which GA is employed to seek for the hyperparameters $\boldsymbol{\theta}$ in the IEK model. For the E2K-DCF, using these different training samples, the optimal hyperparameters for blade and disk were firstly searched by adopting MPGA, and then these decomposed E2K models for blade and disk deformations are derived with different groups of training samples. The SF-CV was thus applied to compute the values of RMSEs for the models of blade and disk deformations. The results of 5 cross validations with 50 training samples, by using DCERSM, DCIEKS and E2K-DCF, are listed in Table 2, in which the average values of $RMSE_b$ and $RMSE_d$ for 5 groups of samples are employed to assess the performance of the derived decomposed-surrogate models of blade and disk deformations, and the unit is 10^{-5} m.

From Table 2, we see that the E2K-DCF has the best modeling accuracy among these three surrogate models based on the analytical results of SF-CV. The reason is that the mean values of RMSEs of blade and disk deformations (0.82×10^{-5} m and 0.81×10^{-5} m) are less than those of the DCERSM (1.17×10^{-5} m and 1.26×10^{-5} m) and DCIEKS (0.86×10^{-5} m and 0.93×10^{-5} m) as shown in last line in Table 2. Therefore, we use the training set of 50 samples to establish the decomposed and coordinated E2K models for blade and disk deformations in this case study. The optimal hyperparameters are computed by adopting MPGA, namely $\boldsymbol{\theta}^{(b)}_{MPGA} = (0.2337, 0.1083, 1.1033, 0.2406, 0.1362)$, and $\boldsymbol{\theta}^{(d)}_{MPGA} = (0.1644, 0.1708, 0.6432, 12.9791, 0.2354)$, corresponding to the minimum values of $\varphi\left(\boldsymbol{\theta}^{(b)}_{MPGA}\right) = 6.9618 \times 10^{-6}$ and $\varphi\left(\boldsymbol{\theta}^{(d)}_{MPGA}\right) = 7.8589 \times 10^{-6}$. The optimizing process of hyperparameters with MPGA is drawn in Fig. 10.

Based on the hyperparameters $\boldsymbol{\theta}^{(b)}_{MPGA}$ and $\boldsymbol{\theta}^{(d)}_{MPGA}$, the decomposed E2K models of turbine blade and disk deformations are built as

$$\begin{aligned} u_b\left(v, P_{out}, T_g, \rho, w\right) &= 9.9501 \times 10^{-2} - 6.0311 \times 10^{-2} v \\ &\quad - 7.8219 \times 10^{-3} P_{out} + 0.9979 T_g \\ &\quad + 0.1165\rho + 0.1484 w + 7.2883 \times 10^{-2} v^2 \\ &\quad - 1.7592 \times 10^{-2} v P_{out} - 1.6441 \times 10^{-2} v T_g \\ &\quad + 5.4348 \times 10^{-2} v\rho + 5.6029 \times 10^{-2} vw \\ &\quad - 2.6252 \times 10^{-3} P_{out}^2 + 5.4222 \times 10^{-3} P_{out} T_g \\ &\quad - 1.6418 \times 10^{-2} P_{out}\rho + 1.0957 \times 10^{-2} P_{out} w \\ &\quad - 7.4779 \times 10^{-2} T_g^2 + 4.1041 \times 10^{-4} T_g \rho \\ &\quad - 8.0127 \times 10^{-3} T_g w - 2.7084 \times 10^{-2} \rho^2 \\ &\quad + 4.8085 \times 10^{-2} \rho w - 1.9793 \times 10^{-3} w^2 \\ &\quad + z_{MPGA,b}\left(v, P_{out}, \rho, T_g, w\right) \end{aligned}$$

$$\begin{aligned} &z_{MPGA,b}\left(v, P_{out}, T_g, \rho, w\right) \\ &\quad = [0.0307, 0.2158, \cdots, -0.1945]_{1\times 50} \end{aligned} \tag{18}$$

$$\begin{aligned} u_d\left(v, P_{out}, T_g, \rho, w\right) &= -8.3635 \times 10^{-2} - 6.6654 \times 10^{-3} v \\ &\quad + 1.4127 \times 10^{-4} P_{out} + 0.7716 T_g \\ &\quad + 0.3853\rho + 0.4750 w + 6.4689 \times 10^{-2} v^2 \\ &\quad - 4.0442 \times 10^{-2} v P_{out} - 1.2955 \times 10^{-2} v T_g \\ &\quad + 1.1280 \times 10^{-2} v\rho + 6.9179 \times 10^{-2} vw \\ &\quad + 1.6609 \times 10^{-2} P_{out}^2 + 1.8619 \times 10^{-2} P_{out} T_g \\ &\quad - 1.4573 \times 10^{-3} P_{out}\rho - 2.5632 \times 10^{-2} P_{out} w \\ &\quad - 4.4458 \times 10^{-2} T_g^2 - 1.1164 \times 10^{-2} T_g \rho \\ &\quad + 5.8452 \times 10^{-3} T_g w + 9.8042 \times 10^{-3} \rho^2 \\ &\quad + 1.6087 \times 10^{-2} \rho w + 7.8391 \times 10^{-2} w^2 \\ &\quad + z_{MPGA,d}\left(v, P_{out}, \rho, T_g, w\right) \end{aligned}$$

$$\begin{aligned} &z_{MPGA,d}\left(v, P_{out}, T_g, \rho, w\right) \\ &\quad = [0.0755, 0.0680, \cdots, -0.1696]_{1\times 50} \end{aligned} \tag{19}$$

where u_b and u_d are the radial deformations of blade and disk, respectively.

Regarding the radial deformation of turbine blisk is defined as the total radial deformation of blade and disk, the coordinated surrogate model is gained as

$$\begin{aligned} u\left(v, P_{out}, T_g, \rho, w\right) = u_b\left(v, P_{out}, T_g, \rho, w\right) \\ + u_d\left(v, P_{out}, T_g, \rho, w\right) \end{aligned} \tag{20}$$

where u is the radial deformation of turbine blisk.

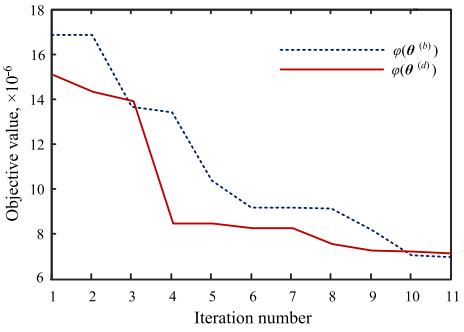

FIGURE 10. Optimizing process of the hyperparameter θ in E2K models of blade and disk with MPGA.

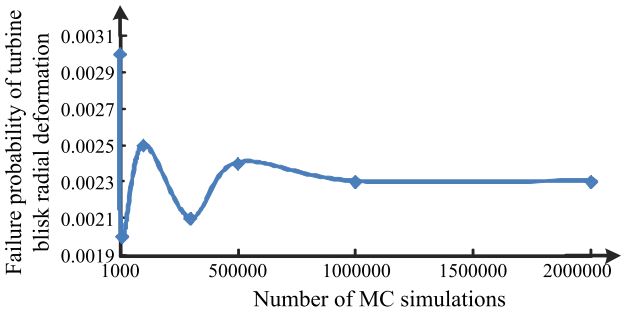

FIGURE 11. The results of convergence analysis with different MC simulations.

In light of Eqs. (11) and (20), the limit state function of turbine blisk radial deformation is derived as

$$\begin{aligned} h\left(v, P_{out}, T_g, \rho, w\right) &= u_{allow} - \left(v, P_{out}, T_g, \rho, w\right) \\ &= u_{allow} - u_b\left(v, P_{out}, T_g, \rho, w\right) \\ &\quad - u_d\left(v, P_{out}, T_g, \rho, w\right) \end{aligned} \tag{21}$$

here, u_{allow} denotes the allowance value of turbine blisk radial deformation selected in term of engineering practice, which is commonly determined by 3 sigma levels.

To investigate the probabilistic failure of turbine blisk, we first conduct different times of MC simulations (10^3, 10^4, 10^5, 3×10^5, 5×10^5, 10^6, 2×10^6) with the derived limit state function Eq. (21) for the convergence assessment [47]. Herein, some sampling methods can be used in MC simulation for structural probabilistic failure analysis, e.g., random sampling, stratified sampling, Sobol sampling, and so forth [49]–[51]. In this paper, we employ MC simulation with purely random sampling to complete the probabilistic failure of turbine blisk radial deformation. The results of convergence analysis with different MC simulations are drawn in Fig. 11.

As shown in Fig. 11, we discover that the failure probabilities of turbine blisk radial deformation are fluctuating when the number of MC simulations is less than 10^6, and these failure probabilities gradually converge to a certain value (i.e., 0.0023) when the number of MC simulations is larger than 10^6. Therefore, we select 10^6 MC simulations to obtain the failure probability of turbine blisk radial deformation. The simulation history diagram and frequency distribution histogram for turbine blisk radial deformation are drawn in Fig. 12.

As revealed in Fig. 12, turbine blisk radial deformation obeys a normal distribution with the mean 2.2884×10^{-3} m and the standard deviation 1.0627×10^{-4} m. In addition, we find 2 300 failures occur in 10^6 MC simulations, so that the failure probability is 0.0023 and the reliability degree is 0.9977 as the allowance value is 2.6072×10^{-3} m.

IV. E2K-DCF VALIDATION

The aim of this section is to validate the modeling and simulation performances of the proposed E2K-DCF by comparing with different surrogate models, which include

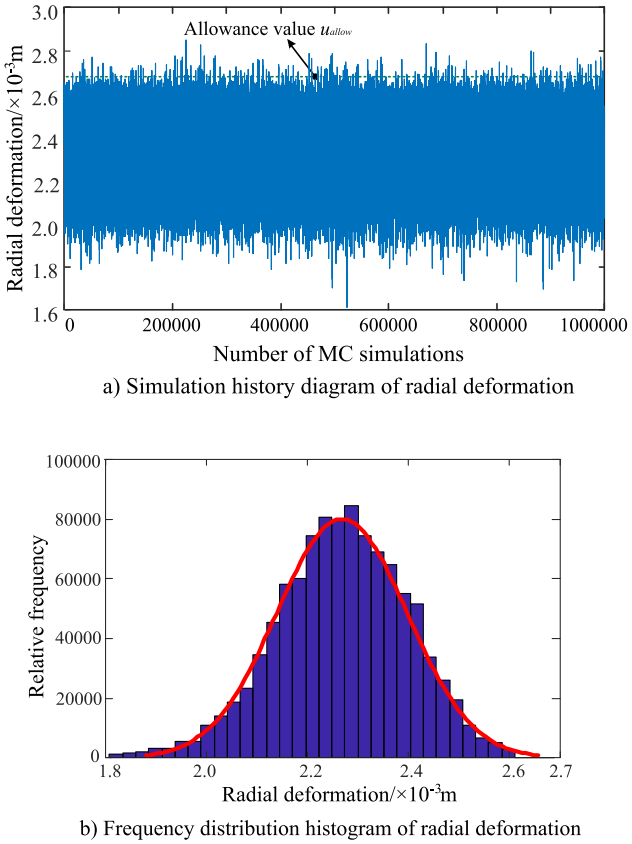

FIGURE 12. Simulation history diagram and frequency distribution histogram of turbine blisk radial deformation.

the DCERSM and DCIEKS. The modeling performance includes learning ability and generalization ability, and the simulation performance involves simulation efficiency and simulation accuracy in dynamic probabilistic analysis of multicomponent structure.

A. MODELING PERFORMANCE

To validate the learning ability of the E2K-DCF model, the 50 input training samples shown in Part C of Section III were inputted in the established E2K models, and then the SF-CV with 5 iterations was used to illustrate the effectiveness by using the mean value of RMSEs for turbine blisk deformation. The results show that the mean value of RMSE of E2K-DCF for turbine blisk deformation (1.63×10^{-5} m) is less than those of the DCERSM and DCIEKS (2.43×10^{-5} m and 1.79×10^{-5} m), which reveals that the developed E2K-DCF has good learning ability and thus high modeling accuracy to some extent. The reason is that (1) the MPGA can avoid the influence of the plateau-like function profile of MLE by flexible and adaptive design space exploration, and breaks the lenition of single population evolution of GA in premature problem by adopting multi populations with different control parameters in parameters optimization and iteration; (2) the ERSM can skillfully process the dynamic response problem by simplifying the response process as one extreme value,

TABLE 3. Simulation performance of E2K-DCF compared with the other methods (including direct simulation, DCERSM and DCIEKS).

Method	Simulation time, s	Failure probability	Reliability degree	Reliability percentage difference, %
Direct simulation	28 800	—	—	—
DCERSM	0.0143	0.0035	0.9965	99.88
DCIEKS	0.0075	0.0016	0.9984	99.92
E2K-DCF	0.0015	0.0023	0.9977	—

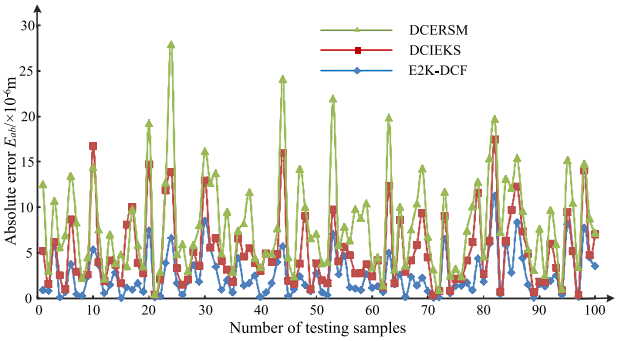

FIGURE 13. The curves of absolute errors of three surrogate models with testing samples.

and make the acquired samples more efficiently reflect the real features of structural dynamic analysis, to improve modeling accuracy; (3) the Kriging model has the capability of global positioning (i.e., $y_{\mathrm{ERSM}}(\boldsymbol{x})$) and local optimization (i.e., $z(\boldsymbol{x})$) in the process modeling, which enhance the accuracy of Kriging modeling to some extent; (4) the DC strategy decomposes the entire multicomponent model into many component-models involving decomposed models and coordinated models, in which a high-nonlinear complex question are divided into numerous sample question with low nonlinearity. The low nonlinearity is easier described and reflected to more precise modeling. The four cases ensure the high-accurate modeling of the proposed E2K-DCF.

To support the generalization ability of E2K-DCF, the testing set of 100 samples is then applied to investigate the prediction performance (generalization ability) with the three surrogate models. The curves of absolute errors of three surrogate models with testing samples are displayed in Fig. 13, in which the results from the direct simulation-based full FE models are regarded as the reference.

As revealed in Fig. 13, the absolute errors of the developed E2K-DCF for 100 testing samples holds the least fluctuating among these three surrogate models. And these errors of the proposed E2K-DCF are close to the true values obtained by the direct simulation-based full FE models, and are smaller than those of other two methods, since the points of absolute errors are closer to the horizontal axis than DCERSM and DCIEKS. Besides, the average absolute error of E2K-DCF is only 2.4862×10^{-6} m which is less than 5.1036×10^{-6} m for DCIEKS and 8.1147×10^{-6} m for DCERSM, and is reduced by 51.29% to that of DCIEKS and 69.36% to that of DCERSM. We can see that (1) relative to DCERSM, the DCIEKS has higher prediction accuracy (better learning ability), which demonstrate that the Kriging model has higher modeling accuracy resulting from its global positioning and local optimization abilities than quadratic polynomials and the hyperparameters in Kriging model can be optimally searched by resolving MLE using the GA rather than gradient descent optimizer; (2) comparing to the DCIEKS, the prediction accuracy of the proposed E2K-DCF is higher due to the strengths of MPGA avoiding the premature problem of single GA in the solution of MLE.

In sum, the proposed E2K-DCF is fully demonstrated to hold high modeling and prediction accuracy, i.e., good learning ability and strong generalization ability.

B. SIMULATION PERFORMANCE

In this section, the simulation performance of the E2K-DCF is assessed from simulation time and accuracy perspectives, in respect of the dynamic reliability evaluation of turbine blisk radial deformation, which is compared to DCERSM and DCIEKS. Herein, the average time for each of these four methods to complete one MC simulation is applied to assess the simulation time, which are shown in column 2 in Table 3. In addition, the failure probability of E2K-DCF with 10^6 MC simulations is treated as the reference to compute the simulation accuracies of DCERSM and DCIEKS, since the prediction accuracy of E2K-DCF is best among the three surrogate models. The simulation accuracy is evaluated by reliability percentage difference, which is determined using the absolute error value of reliability degree between E2K-DCF and other two methods, and is displayed in column 5 in Table 3. It should be noted that all the simulations are finished in the same computational environment (the computer with Processor of Intel®Core™ i5-4590 @ 3.30GHz and RAM (Random Access Memory) of 8 G), and parallel computing was adopted in the computation for the three surrogate models such as DCERSM, DCIEKS and E2K-DCF.

As shown in column 2 in Table 3, using surrogate models such as DCERSM, DCIEKS and E2K-DCF can greatly lighten computing burden, since the surrogate models need less simulations time than the direct simulation method, which can significantly improve the probabilistic simulation of the turbine blisk in efficiency. Among three surrogate models, obviously, the developed E2K-DCF has the highest stimulatingly efficient, owing to the minimum simulation time naturally resulting from the hyperparameters $\boldsymbol{\theta}$ optimized by MPGA and avoiding excessive iterations. As indicated in column 5 Table 3, we find that the simulation accuracy of the proposed E2K-DCF is higher than those of DCERSM

(99.88%) and DCIEKS (99.92%). The major reason is that the MPGA can more precisely find the optimal hyperparameters $\boldsymbol{\theta}$ and make E2K modeling more accurate thanks to avoiding the premature problem of single GA in the solution of MLE. Therefore, the E2K-DCF is verified to hold excellent simulation performance in accuracy and efficiency, which gives us high confidence to apply this method to address the dynamic probabilistic failure analyses of multicomponent structures like turbine blisk in this paper.

V. CONCLUSION

The objective of this paper is to present a novel surrogate modeling approach, enhanced extremum Kriging-based decomposed-coordinated framework (E2K-DCF), for the dynamic probabilistic failure analyses of multicomponent structures with multiple population genetic algorithm (MPGA). In this framework, extremum response surface method (ERSM) is introduced into Kriging model to address the dynamic problem by simplifying the response process as the extreme value in time domain $[0, T]$, which can shorten computational burden and enhance approximate accuracy. MPGA is used to resolve the maximum likelihood equation (MLE) to determine the optimal hyperparameter $\boldsymbol{\theta}$, instead of the gradient descent method. Decomposed-coordinated (DC) strategy is to coordinate the relationship of many analytical objectives in multicomponent structure analyses. The dynamic probabilistic failure of aeroengine turbine blisk radial deformation is evaluated considering fluid-thermal-structural interaction, by running 10^6 Monte Carlo (MC) simulations with purely random sampling, to reveal the advantages of the proposed E2K-DCF from modeling performance and simulation performance by the comparison of methods.

We first implemented the dynamic deterministic analyses of turbine blisk radial deformation to acquire a pool of 150 samples using the close-coupling analysis method, in which 50 samples were treated as the training set to derive surrogate models by using the S-Fold Cross Validation (SF-CV), while the remaining samples were applied to testing the learning ability of these methods. Through the investigation results, we obtain the reliability degree of 0.9977 when the allowance value of turbine blisk radial deformation is 2.6072×10^{-3} m, and discover that the proposed E2K-DCF is superior to the other surrogate models, since the predicted values of this method are closest to those of the direct simulation with the least average absolute error. Furthermore, the E2K-DCF is the most computationally efficient method, owing to its minimum simulation time, as well as has higher analytical accuracy than DCERSM and DCIEKS. Therefore, the E2K-DCF is fully validated to be high modeling performance (modeling and prediction accuracy) and simulation performance (highly-computational efficiency and highly-computational accuracy).

The efforts of this study will provide a useful technique, E2K-DCF, for the probabilistic analysis of multicomponent structures, and also offer a promising insight for handling more engineering problems related to complex structures.

REFERENCES

[1] B. H. Jia and X. D. Zhang, "Study on effect of rotor vibration on tip clearance variation and fast active control of tip clearance," *Adv. Mater. Res.*, vols. 139–141, pp. 2469–2472, Oct. 2010.
[2] C.-Y. Zhang, C. Lu, C.-W. Fei, L.-J. Liu, Y.-S. Choy, and X.-G. Su, "Multiobject reliability analysis of turbine blisk with multidiscipline under multiphysical field interaction," *Adv. Mater. Sci. Eng.*, vol. 2015, Jul. 2015. Art. no. 649046.
[3] H. Azizsoltani and E. Sadeghi, "Adaptive sequential strategy for risk estimation of engineering systems using Gaussian process regression active learning," *Eng. Appl. Artif. Intell.*, vol. 74, pp. 146–165, Sep. 2018.
[4] Z. Zhan, Q. Meng, W. Hu, Y. Sun, F. Shen, and Y. Zhang, "Continuum damage mechanics based approach to study the effects of the scarf angle, surface friction and clamping force over the fatigue life of scarf bolted joints," *Int. J. Fatigue*, vol. 102, pp. 59–78, Sep. 2017.
[5] Z. Zhan, W. Hu, B. Li, Y. Zhang, Q. Meng, and Z. Guan, "Continuum damage mechanics combined with the extended finite element method for the total life prediction of a metallic component," *Int. J. Mech. Sci.*, vols. 124–125, pp. 48–58, May 2017.
[6] Y. Liu, L.-L. Meng, K. Liu, and Y.-M. Zhang, "Chatter reliability of milling system based on first-order second-moment method," *Int. J. Adv. Manuf. Technol.*, vol. 87, nos. 1–4, pp. 801–809, 2016.
[7] S. Adarsh and M. J. Reddy, "Reliability analysis of composite channels using first order approximation and Monte Carlo simulations," *Stochastic Environ. Res. Risk Assessment*, vol. 27, no. 2, pp. 477–487, 2013.
[8] X. Du and Z. Hu, "First order reliability method with truncated random variables," *J. Mech. Des.*, vol. 134, no. 9, 2012, Art. no. 091005.
[9] Y.-G. Zhao and H.-S. A. Alfredo, "On the first-order third-moment reliability method," *Struct. Infrastruct. Eng.*, vol. 8, no. 5, pp. 517–527, 2012.
[10] J. Zhang and X. Du, "A second-order reliability method with first-order efficiency," *J. Mech. Des.*, vol. 132, no. 10, 2010, Art. no. 101006.
[11] S.-P. Zhu, L. Qiang, P. Weiwen, and Z. Xian-Cheng, "Computational-experimental approaches for fatigue reliability assessment of turbine bladed disks," *Int. J. Mech. Sci.*, vols. 142–143, pp. 502–517, Jul. 2018.
[12] S. P. Zhu, Q. Liu, J. Zhou, and Z. Y. Yu, "Fatigue reliability assessment of turbine discs under multi-source uncertainties," *Fatigue Fract. Eng. Mater. Struct.*, vol. 41, no. 6, pp. 1291–1305, Jun. 2018.
[13] S.-P. Zhu, Q. Liu, Q. Lei, and Q. Y. Wang, "Probabilistic fatigue life prediction and reliability assessment of a high pressure turbine disc considering load variations," *Int. J. Damage Mech.*, vol. 27, no. 10, pp. 1569–1588, 2018.
[14] Z.-H. Lu, D.-Z. Hu, and Y.-G. Zhao, "Second-order fourth-moment method for structural reliability," *J. Eng. Mech.*, vol. 143, no. 4, 2017, Art. no. 06016010.
[15] A. Guerine, A. El Hami, L. Walha, T. Fakhfakhb, and M. Haddarb, "Dynamic response of wind turbine gear system with uncertain-but-bounded parameters using interval analysis method," *Renew. Energy*, vol. 113, pp. 679–687, Dec. 2017.
[16] D. Codetta-Raiteri and L. Portinale, "Approaching dynamic reliability with predictive and diagnostic purposes by exploiting dynamic Bayesian networks," *Proc. Inst. Mech. Eng. O, J. Risk Rel.*, vol. 228, no. 5, pp. 488–503, 2014.
[17] W. H. Mo, "Dynamic reliability based on perturbation stochastic finite element," *Appl. Mech. Mater.*, vols. 155–156, pp. 47–50, 2012.
[18] X. Li, C. Gong, L. Gu, W. Gao, Z. Jing, and H. Su, "A sequential surrogate method for reliability analysis based on radial basis function," *Struct. Saf.*, vol. 73, pp. 42–53, Jul. ss2018.
[19] B. Bai, W. Zhang, B. Li, C. Li, and G. C. Bai, "Application of probabilistic and nonprobabilistic hybrid reliability analysis based on dynamic substructural extremum response surface decoupling method for a blisk of the aeroengine," *Int. J. Aerosp. Eng.*, vol. 2017, Mar. 2017, Art. no. 5839620.
[20] J. Cheng, Z. Liu, Z. Wu, X. Li, and J. Tan, "Robust optimization of structural dynamic characteristics based on adaptive Kriging model and CNSGA," *Struct. Multidisciplinary Optim.*, vol. 51, no. 2, pp. 423–437, 2015.

[21] M. Soltani, R. Kulkarni, T. Scheinost, T. Groezinger, and A. Zimmermann, "A novel approach for reliability investigation of LEDs on molded interconnect devices based on FE-analysis coupled to injection molding simulation," *IEEE Access*, vol. 7, pp. 56163–56173, 2019.

[22] C. Fei, W. Tang, G. Bai, and S. Ma, "Dynamic probabilistic design for blade deformation with SVM-ERSM," *Aircr. Eng. Aerosp. Technol.*, vol. 87, no. 4, pp. 312–321, 2015.

[23] C.-W. Fei, Y.-S. Choy, D.-Y. Hu, G.-C. Bai, and W.-Z. Tang, "Transient probabilistic analysis for turbine blade-tip radial clearance with multi-component and multi-physics fields based on DCERSM," *Aerosp. Sci. Technol.*, vol. 50, pp. 62–70, Mar. 2016.

[24] G. Vicario, M. T. Giraudo, and V. Cali, "Kriging modelization in predicting metal sheet elongation," *Qual. Rel. Eng. Int.*, vol. 34, no. 7, pp. 1390–1399, 2018.

[25] J. Vahedi, M. R. Ghasemi, and M. Miri, "An adaptive divergence-based method for structural reliability analysis via multiple Kriging models," *Appl. Math. Model.*, vol. 62, pp. 542–561, Oct. 2018.

[26] C.-Y. Zhang, Z.-S. Yuan, Z. Wang, C.-W. Fei, and C. Lu, "Probabilistic fatigue/creep optimization of turbine bladed disk with fuzzy multi-extremum response surface method," *Materials*, vol. 12, no. 20, p. 3367, 2019.

[27] L. Zhang, Z. Lu, L. Cheng, and Z. Tang, "Emulator model–based analytical solution for reliability sensitivity analysis," *J. Eng. Mech.*, vol. 141, no. 8, 2015, Art. no. 04015016.

[28] Y. Zhang, Y. Liu, X. Yang, and B. Zhao, "An efficient Kriging method for global sensitivity of structural reliability analysis with non-probabilistic convex model," *Proc. Inst. Mech. Eng. O, J. Risk Rel.*, vol. 229, no. 5, pp. 442–455, 2015.

[29] J.-C. Yu and Suprayitno, "Evolutionary reliable regional Kriging surrogate and soft outer array for robust engineering optimization," *IEEE Access*, vol. 5, pp. 16520–16531, 2017.

[30] C.-Y. Zhang, Z. Wang, C.-W. Fei, Z.-S. Yuan, J.-S. Wei, and W.-Z. Tang, "Fuzzy multi-SVR learning model for reliability-based design optimization of turbine blades," *Materials*, vol. 12, no. 15, p. 2341, 2019.

[31] Y. Yin, N. Hong, F. Fei, X. H. Wei, and H. J. Ni, "Nonlinear assembly tolerance design for spatial mechanisms based on reliability methods," *J. Mech. Des.*, vol. 139, no. 3, 2017, Art. no. 032301.

[32] C. Lu, Y.-W. Feng, and C.-W. Fei, "Weighted regression-based extremum response surface method for structural dynamic fuzzy reliability analysis," *Energies*, vol. 12, no. 9, p. 1588, 2019.

[33] C. Lu, Y.-W. Feng, R. P. Leim, and C.-W. Fei, "Improved Kriging with extremum response surface method for structural dynamic reliability and sensitivity analyses," *Aerosp. Sci. Technol.*, vol. 76, pp. 164–175, May 2018.

[34] G. Levitin, "Genetic algorithms in reliability engineering," *Rel. Eng. Syst. Saf.*, vol. 9, no. 91, pp. 975–976, 2005.

[35] J. K. Cochran, S.-M. Horng, and J. W. Fowler, "A multi-population genetic algorithm to solve multi-objective scheduling problems for parallel machines," *Comput. Oper. Res.*, vol. 30, no. 7, pp. 1087–1102, 2003.

[36] X. Gao, H. Yang, L. Lu, and P. Koo, "Wind turbine layout optimization using multi-population genetic algorithm and a case study in Hong Kong offshore," *J. Wind Eng. Ind. Aerodynamics*, vol. 139, pp. 89–99, Apr. 2015.

[37] G. Adomian, "A review of the decomposition method in applied mathematics," *J. Math. Anal. Appl.*, vol. 135, nos. 501–544, Nov. 1988.

[38] J. D. Martin and T. W. Simpson, "Use of Kriging models to approximate deterministic computer models," *AIAA J.*, vol. 43, pp. 853–863, Apr. 2005.

[39] C. Lu, Y.-W. Feng, C.-W. Fei, and X. F. Xue, "Probabilistic analysis method of turbine blisk with multi-failure modes by two-way fluid-thermal-solid coupling," *Proc. Inst. Mech. Eng. C, J. Mech. Eng. Sci.*, vol. 232, no. 16, pp. 2873–2886, 2018.

[40] S. C. Lin and T. Y. Kam, "Probabilistic failure analysis of transversely loaded laminated composite plates using first-order second moment method," *J. Eng. Mech.*, vol. 126, no. 8, pp. 812–820, 2000.

[41] L. J. M. Aslett, T. Nagapetyan, and S. J. Vollmer, "Multilevel Monte Carlo for reliability theory," *Rel. Eng. Syst. Saf.*, vol. 165, pp. 188–196, Sep. 2017.

[42] C.-W. Fei, Y.-S. Choy, D.-Y. Hu, G.-C. Bai, and W.-Z. Tang, "Dynamic probabilistic design approach of high-pressure turbine blade-tip radial running clearance," *Nonlinear Dyn.*, vol. 86, no. 1, pp. 205–223, 2016.

[43] S. B. Lattime and B. M. Steinetz, "High-pressure-turbine clearance control systems: Current practices and future directions," *J. Propuls. Power*, vol. 20, no. 2, pp. 302–311, 2004.

[44] C. Fei and G. Bai, "Extremum selection method of random variable for nonlinear dynamic reliability analysis of turbine blade deformation," *Propuls. Power Res.*, vol. 1, no. 1, pp. 58–63, 2012.

[45] Z. Zhu, Y. Feng, C. Lu, and C. Fei, "Efficient driving plan and validation of aircraft NLG emergency extension system via mixture of reliability models and test bench," *Appl. Sci.*, vol. 9, no. 17, p. 3578, 2019.

[46] K. B. Chilakamarri, "A new method in static structural reliability," *Probabilistic Eng. Mech.*, vol. 17, no. 4, pp. 317–325, 2002.

[47] A. W. Bray, I. B. Abdurakhmanov, A. S. Kadyrov, D. V. Fursa, and I. Bray, "Solving close-coupling equations in momentum space without singularities for charged targets," *Comput. Phys. Commun.*, vol. 212, pp. 55–58, Mar. 2017.

[48] C.-W. Fei, C. Lu, and R. P. Leim, "Decomposed-coordinated surrogate modeling strategy for compound function approximation in a turbine-blisk reliability evaluation," *Aerosp. Sci. Technol.*, vol. 95, Dec. 2019, Art. no. 105466.

[49] F. Ballio and A. Guadagnini, "Convergence assessment of numerical Monte Carlo simulations in groundwater hydrology," *Water Resour. Res.*, vol. 40, no. 4, 2004, Art. no. W04603.

[50] S. Burhenne, D. Jacob, and G. P. Henze, "Sampling based on Sobol'sequences for Monte Carlo techniques applied to building simulations," in *Proc. IBPSA*, Nov. 2011, pp. 14–16.

[51] H. Dai and W. Wang, "Application of low-discrepancy sampling method in structural reliability analysis," *Struct. Saf.*, vol. 31, pp. 55–64, Jan. 2009.

CHENG LU was born in Jining, China, in 1989. He received the B.S. degree in mechanical engineering and automation from Heilongjiang Bayi Agricultural University, China, in 2013, and the M.S. degree in mechanical design and theory from the Harbin University of Science and Technology, China, in 2016. He is currently pursuing the Ph.D. degree with the School of Aeronautics, Northwestern Polytechnical University.

He is the author of more than 10 articles. He holds one patent. His research interests include reliability evaluation, sensitivity analysis, design optimization, and maintenance engineering analysis. He is a Reviewer of the *Journal of Aerospace Science and Technologies*, and *Reliability Engineering and System Safety*.

YUN-WEN FENG was born in Shanghai, China, in 1968. She received the B.S. and M.S. degrees in flight vehicle design and the Ph.D. degree in mechanical design and theory from Northwestern Polytechnical University (NWPU), China, in 1997 and 2000, respectively.

From 1997 to 2000, she was a Lecturer with the School of Aeronautics, NWPU. From 2001 to 2007, she was an Associate Professor with the School of Aeronautics, NWPU. Since 2008, she has been a Professor with the School of Aeronautics, NWPU. She is the author of three books and more than 100 articles. She holds three inventions. Her research interests include reliability engineering and maintenance engineering.

Dr. Feng was a member of the American Institute of Aeronautics and Astronautics (AIAA) and the Chinese Society of Aeronautics and Astronautics (CSAA). She is a Reviewer of the *Chinese Journal of Aeronautics* journal and the *Journal of Systems Engineering and Electronics*.

CHENG-WEI FEI received the B.S. degree in electrical engineering and automation from the Fujian University of Technology, Fuzhou, China, in 2007, and the M.S. degree in aerospace engineering from Shenyang Aerospace University, Shenyang, China, in 2010, and the Ph.D. degree in aerospace engineering from Beihang University, Beijing, China, in 2014.

From 2014 to 2017, he was a Postdoctoral Fellow (Hong Kong Scholars) of the Department of Mechanical Engineering, The Hong Kong Polytechnic University, Hong Kong. From 2017 to 2018, he was a Research Fellow of the Department of Mechanical and Aerospace Engineering, The Hong Kong University of Science and Technology, Hong Kong. Since 2018, he has been a Research Professor with the Department of Aeronautics and Astronautics, Fudan University, Shanghai, China. He is the author of one book and more than 100 articles. He holds three inventions. His research interests include surrogate model, multidisciplinary design optimization (MDO), reliability-based design optimization (RBDO), and structural health monitoring with machine/deep learning for aircrafts and aero-engines.

Dr. Fei is a member of the American Institute of Aeronautics and Astronautics (AIAA), the Chinese Society of Aeronautics and Astronautics (CSAA), and the American Society of Mechanical Engineers (ASME). He was a recipient of the National Excellent Doctoral Dissertation, in 2016, the Hong Kong Scholars Award, in 2016, and the Academic Scholarship of the Chinese Ministry of Education for Ph.D. degree students, in 2012, and the National Graduate Scholarship of China, in 2012. He is the Reviewer of more than 10 journals such as IEEE Access, *Nonlinear Dynamics*, *Mechanical System and Signal Processing*, *Aerospace Science and Technology*, *Aerospace Science and Technology*, and *Reliability Engineering and System Safety*. He is the Leader Guest Editor of *Advances in Acoustics and Vibration and Advances in Mechanical Engineering*.

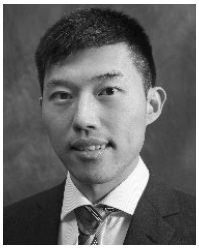

SIQI BU (S'11–M'12–SM'17) received the Ph.D. degree in electric power and energy research cluster from the Queen's University of Belfast, Belfast, U.K., in 2012.

He continued the Postdoctoral research work with the Queen's University of Belfast before entering industry. Subsequently, he joined National Grid, U.K., as a Senior Power System Engineer and then became an experienced U.K. National Transmission System Planner and Operator. He is an Assistant Professor with The Hong Kong Polytechnic University, Hong Kong, and also a Chartered Engineer with the U.K. Royal Engineering Council, London, U.K. His research interests include power system stability analysis and operation control, including wind power generation, PEV, HVDC, FACTS, ESS, and VSG.

Dr. Bu has received various prizes due to excellent performances and outstanding contributions in operational and commissioning projects during the employment with National Grid, U.K. He was a recipient of Outstanding Reviewer Award from the Ieee Transactions on Sustainable Energy, the IEEE Transactions on Power Systems, *Renewable Energy*, and the *International Journal of Electrical Power and Energy Systems*. He is an Associate Editor of IEEE Access, a Guest Editor of *IET Renewable Power Generation*, and an Editor of *Protection and Control of Modern Power Systems*.